

A Semi-Linear Approximation of the First-Order Marcum Q -function with Application to Predictor Antenna Systems

Hao Guo, *Student Member, IEEE*, Behrooz Makki, *Senior Member, IEEE*, Mohamed-Slim Alouini, *Fellow, IEEE*, and Tommy Svensson, *Senior Member, IEEE*

Abstract—First-order Marcum Q -function is observed in various problem formulations. However, it is not an easy-to-handle function. For this reason, in this paper, we first present a semi-linear approximation of the Marcum Q -function. Our proposed approximation is useful because it simplifies, e.g., various integral calculations including Marcum Q -function as well as different operations such as parameter optimization. Then, as an example of interest, we apply our proposed approximation approach to the performance analysis of predictor antenna (PA) systems. Here, the PA system is referred to as a system with two sets of antennas on the roof of a vehicle. Then, the PA positioned in the front of the vehicle can be used to improve the channel state estimation for data transmission of the receive antenna that is aligned behind the PA. Considering spatial mismatch due to the mobility, we derive closed-form expressions for the instantaneous and average throughput as well as the throughput-optimized rate allocation. As we show, our proposed approximation scheme enables us to analyze PA systems with high accuracy. Moreover, our results show that rate adaptation can improve the performance of PA systems with different levels of spatial mismatch.

Index Terms—Backhaul, channel state information (CSI), integrated access and backhaul (IAB), linear approximation, Marcum Q -function, mobility, mobile relay, outage probability, predictor antenna, rate adaptation, spatial correlation, throughput.

I. INTRODUCTION

The first-order Marcum Q -function¹ is defined as [1, Eq. (1)]

$$Q_1(\alpha, \beta) = \int_{\beta}^{\infty} x e^{-\frac{x^2 + \alpha^2}{2}} I_0(x\alpha) dx, \quad (1)$$

where $\alpha, \beta \geq 0$ and $I_n(x) = \left(\frac{x}{2}\right)^n \sum_{i=0}^{\infty} \frac{(\frac{x}{2})^{2i}}{i! \Gamma(n+i+1)}$ is the n -order modified Bessel function of the first kind, and $\Gamma(z) = \int_0^{\infty} x^{z-1} e^{-x} dx$ represents the Gamma function. Reviewing the literature, the Marcum Q -function has appeared in many areas such as statistics/signal detection [2], and in the performance analysis of different setups such as temporally

H. Guo and T. Svensson are with the Department of Electrical Engineering, Chalmers University of Technology, 41296 Gothenburg, Sweden (email: hao.guo@chalmers.se; tommy.svensson@chalmers.se).

B. Makki is with Ericsson Research, 41756 Gothenburg, Sweden (email: behrooz.makki@ericsson.com).

M.-S. Alouini is with the King Abdullah University of Science and Technology, Thuwal 23955-6900, Saudi Arabia (e-mail: slim.alouini@kaust.edu.sa).

¹To simplify the analysis, our paper concentrates on the approximation of the first-order Marcum- Q function. However, our approximation technique can be easily extended to the cases with different orders of Marcum Q -function.

correlated channels [3], spatially correlated channels [4], free-space optical (FSO) links [5], relay networks [6], as well as cognitive radio and radar systems [7]–[26]. However, in these applications, the presence of the Marcum Q -function makes the mathematical analysis challenging, because it is difficult to manipulate with no closed-form expressions especially when it appears in parameter optimizations and integral calculations. For this reason, several methods have been developed in [1], [27]–[39] to bound/approximate the Marcum Q -function. For example, [27], [28] have proposed modified forms of the function, while [29], [30] have derived exponential-type bounds which are good for the bit error rate analysis at high signal-to-noise ratios (SNRs). Other types of bounds are expressed by, e.g., error function [35] and Bessel functions [36]–[38]. Some alternative methods have been also proposed in [1], [31]–[34]. Although each of these approximation/bounding techniques are fairly tight for their considered problem formulation, they are still based on difficult functions, or have complicated summation/integration formations, which may be not easy to deal with in, e.g., integral calculations and parameter optimizations.

In this paper, we first propose a simple semi-linear approximation of the first-order Marcum Q -function (Lemma 1, Corollaries 1-2). As we explain in the following (Lemmas 1–4), in contrast to the schemes of [1], [27]–[39], our proposed approximation is not tight at the tails of the Marcum Q -function. Therefore, it is not useful in, e.g., error probability-based problem formulations. On the other hand, the advantages of our proposed approximation method, compared to [1], [27]–[39], are 1) its simplicity, and 2) tightness in the moderate values of the function. This is important because, as observed in, e.g., [1], [3]–[8], [11], [14], [16], [17], [19]–[24], [27], in different applications, the Marcum Q -function is typically combined with other functions which tend to zero at the tails of the Marcum Q -function. In such cases, the inaccuracy of the approximation at the tails does not affect the tightness of the final analysis. Thus, our proposed scheme provides tight and simple approximation results for different problem formulations such as capacity calculation [4], [8], throughput/average rate derivation [3], [5], [6], energy detection of unknown signals over various multipath fading channels [14], [16], [17], as well as performance evaluation of non-coherent receivers in radar systems [18]. Also, the simplicity of the approximation method makes it possible to perform further analysis such as parameter optimization and to obtain intuitive insights from the derivations.

To demonstrate the usefulness of the proposed approximation technique in communication systems, we analyze the performance of predictor antenna (PA) systems in presence of spatial mismatch. Here, the PA system is referred to as a setup with two (sets of) antennas on the roof of a vehicle. The PA positioned in the front of a vehicle can be used to improve the channel state estimation for downlink data reception at the receive antenna (RA) on the vehicle that is aligned behind the PA [40]–[48].

The feasibility of PA setups, which are of interest particularly in public transport systems such as trains and buses, but potentially also for the more design-constrained cars, has been previously shown through experimental tests [40]–[46]. Particularly, as shown in testbed implementations, e.g., [42] and [45], with a two-antenna PA setup a normalised mean square error of around -10 dB can be obtained for speeds up to 50 km/h, with measured predictions horizons up to three times the wavelengths. This is by an order of magnitude better than state-of-the-art Kalman prediction-based systems [49], [50] with prediction horizon limited to 0.1–0.3 times the wavelength. Moreover, the European project deliverables, e.g., ARTIST4G project [51, Chapter 2], METIS project [52, P. 107] and 5GCAR project [53, Chapter 3], have well addressed the feasibility of the PA concept in network-level design. Finally, different works have analyzed the PA system in both frequency division duplex (FDD) [42], [43], [45] and time division duplex (TDD) [41], [46] systems, with some developments on addressing the system challenges such as antenna coupling [44], [47], spatial mismatch [47], [48], and spectrum underutilization [54], [55].

Among the challenges of the PA system is the spatial mismatch. If the RA does not arrive in the same position as the PA, the actual channel for the RA would not be identical to the one experienced by the PA before. Such inaccurate channel state information (CSI) estimation will affect the system performance considerably at moderate/high speeds [41], [48].

In this paper, we address the spatial mismatch problem by implementing adaptive rate allocation. In our proposed setup, the instantaneous CSI provided by the PA is used to adapt the data rate of the signals sent to the RA from the base station (BS). The problem is cast in the form of throughput maximization. Particularly, we use our developed approximation approach to derive closed-form expressions for the instantaneous and average throughput as well as the optimal rate allocation maximizing the throughput (Lemma 4). Moreover, we study the effect of different parameters such as the antennas distance, the vehicle speed, and the processing delay of the BS on the performance of PA setups.

Our paper is different from the state-of-the-art literature because the proposed semi-linear approximation of the first-order Marcum Q -function and the derived closed-form expressions for the considered integrals have not been presented by, e.g., [1]–[48]. Also, as opposed to [40]–[47], we perform analytical evaluations on the system performance with CSIT (T: at the transmitter)-based rate optimization to mitigate the effect of the spatial mismatch. Moreover, compared to our preliminary results in [48], this paper develops the semi-

linear approximation method for the Marcum Q -function, and uses our proposed approximation method to analyze the performance of the PA system. Also, we perform deep analysis of the effect of various parameters, such as imperfect CSIT feedback schemes, and processing delay of the BS on the system performance.

The simulation and the analytical results indicate that the proposed semi-linear approximation is useful for the mathematical analysis of different Marcum Q -function-based problem formulations. Particularly, our approximation method enables us to represent different Marcum Q -function-based integrations and optimizations in closed-form. Considering the PA system, our derived analytical results show that adaptive rate allocation can considerably improve the performance of the PA system in the presence of spatial mismatch. Finally, with different levels of channel estimation, our results show that there exists an optimal speed for the vehicle optimizing the throughput/outage probability, and the system performance is sensitive to the vehicle speed/processing delay as the speed moves away from its optimal value.

This paper is organized as follows. In Section II, we present our proposed semi-linear approximation of the first-order Marcum Q -function, and derive closed-form solutions for some integrals of interest. Section III deals with the application of the approximation in the PA system, deriving closed-form expressions for the optimal rate adaptation, the instantaneous throughput as well as the expected throughput. In this way, Sections II and III demonstrate examples on how the proposed approximation can be useful in, respectively, expectation- and optimization-based problem formulations involving the Marcum Q -function. Concluding remarks are provided in Section IV.

II. APPROXIMATION OF THE FIRST-ORDER MARCUM Q -FUNCTION

In this section, we present our semi-linear approximation of the cumulative distribution function (CDF) in the form of $y(\alpha, \beta) = 1 - Q_1(\alpha, \beta)$. The idea of this proposed approximation is to use one point and its corresponding slope in that point to create a line approximating the CDF. The approximation method is summarized in Lemma 1 as follows.

Lemma 1. *The CDF of the form $y(\alpha, \beta) = 1 - Q_1(\alpha, \beta)$ can be semi-linearly approximated as $Y(\alpha, \beta) \simeq \mathcal{Z}(\alpha, \beta)$ where*

$$\mathcal{Z}(\alpha, \beta) = \begin{cases} 0, & \text{if } \beta < c_1 \\ \frac{\alpha + \sqrt{\alpha^2 + 2}}{2} e^{-\frac{1}{2} \left(\alpha^2 + \left(\frac{\alpha + \sqrt{\alpha^2 + 2}}{2} \right)^2 \right)} \times \\ I_0 \left(\alpha \frac{\alpha + \sqrt{\alpha^2 + 2}}{2} \right) \times \left(\beta - \frac{\alpha + \sqrt{\alpha^2 + 2}}{2} \right) + \\ 1 - Q_1 \left(\alpha, \frac{\alpha + \sqrt{\alpha^2 + 2}}{2} \right), & \text{if } c_1 \leq \beta \leq c_2 \\ 1, & \text{if } \beta > c_2, \end{cases} \quad (2)$$

with

$$c_1(\alpha) = \max \left(0, \frac{\alpha + \sqrt{\alpha^2 + 2}}{2} + \frac{Q_1 \left(\alpha, \frac{\alpha + \sqrt{\alpha^2 + 2}}{2} \right) - 1}{\frac{\alpha + \sqrt{\alpha^2 + 2}}{2} e^{-\frac{1}{2} \left(\alpha^2 + \left(\frac{\alpha + \sqrt{\alpha^2 + 2}}{2} \right)^2 \right)} I_0 \left(\alpha \frac{\alpha + \sqrt{\alpha^2 + 2}}{2} \right)} \right), \quad (3)$$

$$c_2(\alpha) = \frac{\alpha + \sqrt{\alpha^2 + 2}}{2} + \frac{Q_1 \left(\alpha, \frac{\alpha + \sqrt{\alpha^2 + 2}}{2} \right)}{\frac{\alpha + \sqrt{\alpha^2 + 2}}{2} e^{-\frac{1}{2} \left(\alpha^2 + \left(\frac{\alpha + \sqrt{\alpha^2 + 2}}{2} \right)^2 \right)} I_0 \left(\alpha \frac{\alpha + \sqrt{\alpha^2 + 2}}{2} \right)}. \quad (4)$$

Proof. We aim to approximate the CDF in the range $y \in [0, 1]$ by

$$y - y_0 = m(x - x_0), \quad (5)$$

where $\mathcal{C} = (x_0, y_0)$ is a point on the CDF curve and m is the slope at point \mathcal{C} of $y(\alpha, \beta)$. Then, the parts of the line outside this region are replaced by $y = 0$ and $y = 1$ (see Fig. 1).

To obtain a good approximation of the CDF, we select the point \mathcal{C} by solving

$$x = \arg_t \left\{ \frac{\partial^2 (1 - Q_1(\alpha, t))}{\partial t^2} = 0 \right\}, \quad (6)$$

because the function is symmetric around this point, and (6) gives the best fit for a linear function. Then, using the derivative of the first-order Marcum Q -function with respect to x [56, Eq. (2)]

$$\frac{\partial Q_1(\alpha, x)}{\partial x} = -x e^{-\frac{\alpha^2+x^2}{2}} I_0(\alpha x), \quad (7)$$

(6) is equivalent to

$$x = \arg_x \left\{ \frac{\partial \left(x e^{-\frac{\alpha^2+x^2}{2}} I_0(\alpha x) \right)}{\partial x} = 0 \right\}. \quad (8)$$

Using the approximation $I_0(x) \simeq \frac{e^x}{\sqrt{2\pi x}}$ [57, Eq. (9.7.1)] and writing

$$\begin{aligned} \frac{\partial \left(\sqrt{\frac{x}{2\pi\alpha}} e^{-\frac{(x-\alpha)^2}{2}} \right)}{\partial x} &= 0 \\ \Rightarrow \frac{1}{\sqrt{2\pi\alpha}} \left(\frac{e^{-\frac{(x-\alpha)^2}{2}}}{2\sqrt{x}} + \sqrt{x} e^{-\frac{(x-\alpha)^2}{2}} (\alpha - x) \right) &= 0 \\ \Rightarrow 2x^2 - 2\alpha x - 1 &= 0, \end{aligned} \quad (9)$$

we obtain

$$x = \frac{\alpha + \sqrt{\alpha^2 + 2}}{2}, \quad (10)$$

since $x \geq 0$. In this way, we find the point

$$\mathcal{C} = \left(\frac{\alpha + \sqrt{\alpha^2 + 2}}{2}, 1 - Q_1 \left(\alpha, \frac{\alpha + \sqrt{\alpha^2 + 2}}{2} \right) \right). \quad (11)$$

To calculate the slope m at the point \mathcal{C} , we plug (10) into (7) leading to

$$m = \frac{\alpha + \sqrt{\alpha^2 + 2}}{2} \times e^{-\frac{1}{2} \left(\alpha^2 + \left(\frac{\alpha + \sqrt{\alpha^2 + 2}}{2} \right)^2 \right)} I_0 \left(\alpha \frac{\alpha + \sqrt{\alpha^2 + 2}}{2} \right). \quad (12)$$

Finally, using (5), (10) and (12), the CDF $y(\alpha, \beta) = 1 - Q_1(\alpha, \beta)$ can be approximated as in (2). Note that, because the CDF is limited to the range $[0, 1]$, the boundaries c_1 and c_2 in (2) are obtained by setting $y = 0$ and $y = 1$ which leads to the semi-linear approximation as given in (2). ■

To further simplify the calculation, considering different ranges of α , the approximation (2) can be simplified as stated in the following corollaries.

Corollary 1. For moderate/large values of α , we have $y(\alpha, \beta) \simeq \tilde{\mathcal{Z}}(\alpha, \beta)$ where

$$\tilde{\mathcal{Z}}(\alpha, \beta) \simeq \begin{cases} 0, & \text{if } \beta < \frac{-\frac{1}{2}(1 - e^{-\alpha^2} I_0(\alpha^2))}{\alpha e^{-\alpha^2} I_0(\alpha^2)} + \alpha \\ \alpha e^{-\alpha^2} I_0(\alpha^2)(\beta - \alpha) + \frac{1}{2}(1 - e^{-\alpha^2} I_0(\alpha^2)), & \text{if } \frac{-\frac{1}{2}(1 - e^{-\alpha^2} I_0(\alpha^2))}{\alpha e^{-\alpha^2} I_0(\alpha^2)} + \alpha \leq \beta \\ \leq \frac{1 - \frac{1}{2}(1 - e^{-\alpha^2} I_0(\alpha^2))}{\alpha e^{-\alpha^2} I_0(\alpha^2)} + \alpha, & \text{if } \beta > \frac{1 - \frac{1}{2}(1 - e^{-\alpha^2} I_0(\alpha^2))}{\alpha e^{-\alpha^2} I_0(\alpha^2)} + \alpha. \end{cases} \quad (13)$$

$$\stackrel{(a)}{\simeq} \begin{cases} 0, & \text{if } \beta < \check{c}_1 \\ \frac{1}{\sqrt{2\pi}}(\beta - \alpha) + \frac{1}{2} \left(1 - \frac{1}{\sqrt{2\pi\alpha^2}} \right), & \text{if } \check{c}_1 \leq \beta \leq \check{c}_2 \\ 1, & \text{if } \beta > \check{c}_2, \end{cases} \quad (14)$$

with \check{c}_1 and \check{c}_2 given in (18) and (19), respectively.

Proof. Using (10) for moderate/large values of α , we have $x \simeq \alpha$ and

$$\tilde{c}_1 = \frac{-\frac{1}{2}(1 - e^{-\alpha^2} I_0(\alpha^2))}{\alpha e^{-\alpha^2} I_0(\alpha^2)} + \alpha, \quad (15)$$

$$\tilde{c}_2 = \frac{1 - \frac{1}{2}(1 - e^{-\alpha^2} I_0(\alpha^2))}{\alpha e^{-\alpha^2} I_0(\alpha^2)} + \alpha, \quad (16)$$

which leads to (13). Note that in (13) we have used the fact that [58, Eq. (A-3-2)]

$$Q_1(\alpha, \alpha) = \frac{1}{2} \left(1 + e^{-\alpha^2} I_0(\alpha^2) \right). \quad (17)$$

Finally, (a) is obtained by using the approximation $I_0(x) \simeq \frac{e^x}{\sqrt{2\pi x}}$ where

$$\check{c}_1 = -\frac{\sqrt{2\pi}}{2} \left(1 - \frac{1}{\sqrt{2\pi\alpha^2}} \right) + \alpha, \quad (18)$$

and

$$\check{c}_2 = \sqrt{2\pi} - \frac{\sqrt{2\pi}}{2} \left(1 - \frac{1}{\sqrt{2\pi\alpha^2}} \right) + \alpha. \quad (19)$$

■

Corollary 2. For small values of α , we have $y(\alpha, \beta) \simeq \hat{Z}(\alpha, \beta)$ with

$$\hat{Z}(\alpha, \beta) \simeq \begin{cases} 0, & \text{if } \beta < \hat{c}_1 \\ \frac{\alpha+\sqrt{2}}{2} e^{-\frac{\alpha^2+(\frac{\alpha+\sqrt{2}}{2})^2}{2}} \times \\ I_0\left(\frac{\alpha(\alpha+\sqrt{2})}{2}\right) (\beta - \frac{\alpha+\sqrt{2}}{2}) + \\ 1 - Q_1\left(\alpha, \frac{\alpha+\sqrt{2}}{2}\right), & \text{if } \hat{c}_1 \leq \beta \leq \hat{c}_2 \\ 1, & \text{if } \beta > \hat{c}_2 \end{cases} \quad (20)$$

with \hat{c}_1 and \hat{c}_2 given in (21) and (22), respectively.

Proof. Using (10) for small values of α , we have $x \simeq \frac{\alpha+\sqrt{2}}{2}$, which leads to

$$\hat{c}_1 = \frac{-1 + Q_1\left(\alpha, \frac{\alpha+\sqrt{2}}{2}\right)}{\left(\frac{\alpha+\sqrt{2}}{2}\right)^2 e^{-\frac{\alpha^2+(\frac{\alpha+\sqrt{2}}{2})^2}{2}} I_0\left(\frac{\alpha(\alpha+\sqrt{2})}{2}\right)} + \alpha, \quad (21)$$

and

$$\hat{c}_2 = \frac{Q_1\left(\alpha, \frac{\alpha+\sqrt{2}}{2}\right)}{\left(\frac{\alpha+\sqrt{2}}{2}\right)^2 e^{-\frac{\alpha^2+(\frac{\alpha+\sqrt{2}}{2})^2}{2}} I_0\left(\frac{\alpha(\alpha+\sqrt{2})}{2}\right)} + \alpha, \quad (22)$$

and simplifies (2) to (20). ■

To illustrate these semi-linear approximations, Fig. 1 shows the CDF $y(\alpha, \beta) = 1 - Q_1(\alpha, \beta)$ for both small and large values of α , and compares the exact CDF with the approximation schemes of Lemma 1 and Corollaries 1-2. From Fig. 1, we can observe that Lemma 1 is tight for a broad range of α and moderate values of β . Moreover, the tightness is improved as α decreases. Also, Corollaries 1-2 provide good approximations for large and small values of α , respectively. Then, the proposed approximations are not tight at the tails of the CDF. However, as observed in [1], [3]-[8], [11], [14], [16], [17], [19]-[24], [27] and in the following, in different applications, the Marcum Q -function is normally combined with other functions which tend to zero of the tails of the CDF. In such cases, the inaccuracy of the approximation at the tails does not affect the tightness of the final result.

As an example, we first consider a general integral in the form of

$$G(\alpha, \rho) = \int_{\rho}^{\infty} e^{-nx} x^m (1 - Q_1(\alpha, x)) dx \quad \forall n, m, \alpha, \rho > 0. \quad (23)$$

Such an integral has been observed in various applications, e.g., in bit-error-probability evaluation of a Rayleigh fading channel [7, eq. (1) (13)], in energy detection of unknown signals over various multipath fading channels [16, eq. (2)], in capacity analysis with channel inversion and fixed rate

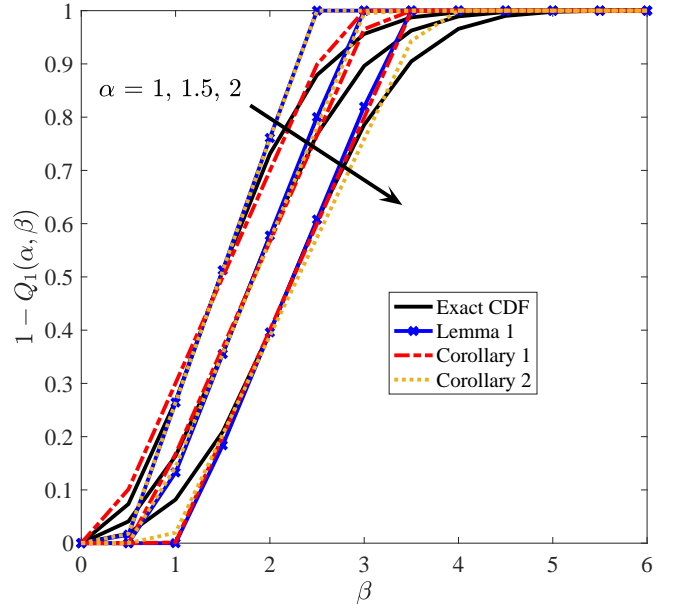


Fig. 1. Illustration of the semi-linear approximation with Lemma 1, and Corollaries 1-2. For each value of $\alpha \in [1, 1.5, 2]$, the approximated results obtained by Lemma 1 and Corollaries 1-2 are compared with the exact value for a broad range of β .

over correlated Nakagami fading [17, eq. (1)], in performance evaluation of incoherent receivers in radar systems [18, eq. (3)], and in error probability analysis of diversity receivers [34, eq. (1)]. However, depending on the values of n, m and ρ , (23) may have no closed-form expression. Using Lemma 1, $G(\alpha, \rho)$ can be approximated in closed-form as presented in Lemma 2.

Lemma 2. The integral (23) is approximately given by

$$G(\alpha, \rho) \simeq \begin{cases} \frac{\Gamma(m+1, n\rho) n^{-m-1}}{\Gamma(m+1, n\check{c}_2) n^{-m-1}}, & \text{if } \rho \geq \check{c}_2 \\ \left(-\frac{\alpha}{\sqrt{2\pi}} + 0.5 * \left(1 - \frac{1}{\sqrt{2\pi\alpha^2}} \right) \right) \times n^{-m-1} \times \\ (\Gamma(m+1, n \max(\check{c}_1, \rho)) - \Gamma(m+1, n\check{c}_2)) + \\ (\Gamma(m+2, n \max(\check{c}_1, \rho)) - \Gamma(m+2, n\check{c}_2)) \times \\ \frac{n^{-m-2}}{\sqrt{2\pi}}, & \text{if } \rho < \check{c}_2, \end{cases} \quad (24)$$

where $\Gamma(s, x) = \int_x^{\infty} t^{s-1} e^{-t} dt$ is the upper incomplete gamma function [57, Eq. 6.5.1].

Proof. See Appendix A. ■

As a second integration example of interest, consider

$$T(\alpha, m, a, \theta_1, \theta_2) = \int_{\theta_1}^{\theta_2} e^{-mx} \log(1 + ax) Q_1(\alpha, x) dx \quad \forall m > 0, a, \alpha, \theta_1, \theta_2 \quad (25)$$

with $\theta_2 > \theta_1 \geq 0$, which does not have a closed-form expression for different values of m, a, α . This type of integral is interesting as it could be used to analyze the expected performance of outage-limited systems, e.g, the considered integral in the shape of [7, eq. (1) (13)], [16, eq. (2)], [18, eq.

(3)], and [34, eq. (1)], applied in the analysis of the outage-limited throughput, i.e., when the outage-limited throughput $\log(1+ax)Q_1(\alpha, x)$ [59, p. 2631] [60, Theorem 6] [61, Eq. (9)] is averaged over fading statistics. Then, using Lemma 1, (25) can be approximated in closed-form as follows.

Lemma 3. *The integral (25) is approximately given by*

$$T(\alpha, m, a, \theta_1, \theta_2) \simeq \begin{cases} \mathcal{F}_1(\theta_2) - \mathcal{F}_1(\theta_1), & \text{if } 0 \leq \theta_1 < \theta_2 < c_1 \\ \mathcal{F}_1(c_1) - \mathcal{F}_1(\theta_1) + \mathcal{F}_2(\max(c_2, \theta_2)) - \mathcal{F}_2(c_1), & \text{if } \theta_1 < c_1, \theta_2 \geq c_1 \\ \mathcal{F}_2(\max(c_2, \theta_2)) - \mathcal{F}_2(c_1), & \text{if } \theta_1 > c_1 \\ 0, & \text{if } \theta_1 > c_2, \end{cases} \quad (26)$$

where c_1 and c_2 are given by (3) and (4), respectively. Moreover,

$$\mathcal{F}_1(x) \doteq \frac{1}{m} \left(-e^{\frac{m}{a}} \text{E}_1 \left(mx + \frac{m}{a} \right) - e^{-mx} \log(ax + 1) \right), \quad (27)$$

and

$$\mathcal{F}_2(x) \doteq e^{-mx} \left((mn_2 - an_2 - amn_1) e^{\frac{m(ax+1)}{a}} \right. \\ \left. - \text{E}_1 \left(\frac{m(ax+1)}{a} \right) - a(mn_2x + n_2 + mn_1) \right. \\ \left. \log(ax + 1) - an_2 \right), \quad (28)$$

with

$$n_1 = 1 + \frac{\alpha + \sqrt{\alpha^2 + 2}}{2} e^{-\frac{1}{2} \left(\alpha^2 + \left(\frac{\alpha + \sqrt{\alpha^2 + 2}}{2} \right)^2 \right)} \times \\ I_0 \left(\alpha + \sqrt{\alpha^2 + 2} \right) \times \frac{\alpha + \sqrt{\alpha^2 + 2}}{2} - \\ 1 + Q_1 \left(\alpha, \frac{\alpha + \sqrt{\alpha^2 + 2}}{2} \right), \quad (29)$$

and

$$n_2 = -\frac{\alpha + \sqrt{\alpha^2 + 2}}{2} e^{-\frac{1}{2} \left(\alpha^2 + \left(\frac{\alpha + \sqrt{\alpha^2 + 2}}{2} \right)^2 \right)} \times \\ I_0 \left(\alpha + \sqrt{\alpha^2 + 2} \right). \quad (30)$$

In (27) and (28), $\text{E}_1(x) = \int_x^\infty \frac{e^{-t}}{t} dt$ is the Exponential Integral function [57, p. 228, (5.1.1)].

Proof. See Appendix B. \blacksquare

Finally, setting $m = 0$ in (25), i.e.,

$$T(\alpha, 0, a, \theta_1, \theta_2) = \int_{\theta_1}^{\theta_2} \log(1+ax)Q_1(\alpha, x)dx, \forall a, \alpha, \quad (31)$$

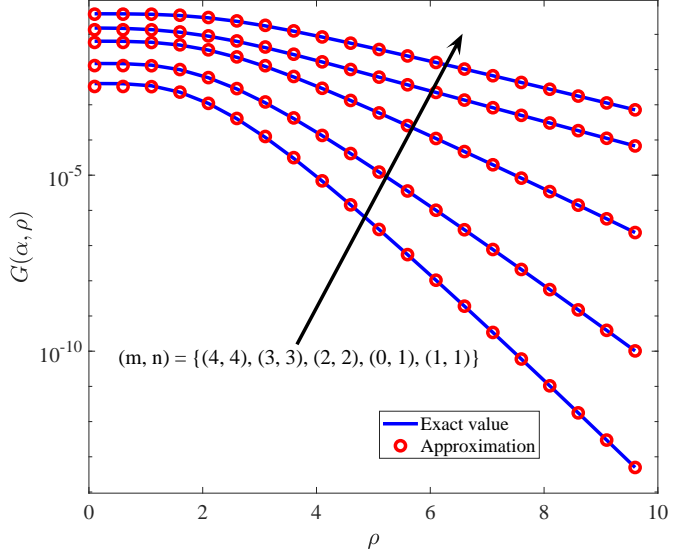


Fig. 2. The integral (23) involving Marcum Q -function. Solid lines are exact values while crosses are the results obtained from Lemma 2, $\alpha = 2$, $(m, n) = \{(4, 4), (3, 3), (2, 2), (0, 1), (1, 1)\}$.

one can follow the same procedure in (25) to approximate (31) as

$$T(\alpha, 0, a, \theta_1, \theta_2) \simeq \begin{cases} \mathcal{F}_3(\theta_2) - \mathcal{F}_3(\theta_1), & \text{if } 0 \leq \theta_1 < \theta_2 < c_1 \\ \mathcal{F}_3(c_1) - \mathcal{F}_3(\theta_1) + \mathcal{F}_4(\max(c_2, \theta_2)) - \mathcal{F}_4(c_1), & \text{if } \theta_1 < c_1, \theta_2 \geq c_1 \\ \mathcal{F}_4(\max(c_2, \theta_2)) - \mathcal{F}_4(c_1), & \text{if } \theta_1 > c_1 \\ 0, & \text{if } \theta_1 > c_2, \end{cases} \quad (32)$$

with c_1 and c_2 given by (3) and (4), respectively. Also,

$$\mathcal{F}_3 = \frac{(ax+1)(\log(ax+1)-1)}{a}, \quad (33)$$

and

$$\mathcal{F}_4 = \frac{n_2 ((2a^2x^2 - 2)\log(ax+1) - a^2x^2 + 2ax)}{4a^2} + \\ \frac{n_1(ax+1)(\log(ax+1)-1)}{a}, \quad (34)$$

where n_1 and n_2 are given by (29) and (30), respectively.

In Figs. 2 and 3, we evaluate the tightness of the approximations in Lemmas 2, 3 and (32), for different values of m, n, ρ, a and α . From the figures, it can be observed that the approximation schemes of Lemmas 2-3 and (32) are very tight for different parameter settings, while our proposed semi-linear approximation makes it possible to represent the integrals in closed-form. In this way, although the approximation (2) is not tight at the tails of the CDF, it gives tight approximation results when it appears in different integrals (Lemmas 2-3) with the Marcum- Q function combined with other functions tending to zero at the tails of the function. Also, as we show in Section III, the semi-linear approximation scheme is efficient in optimization problems involving the Marcum Q -function.

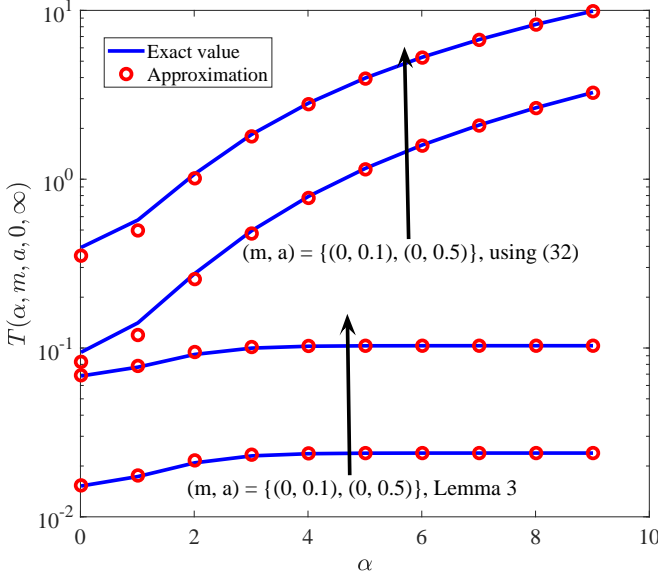


Fig. 3. The integral (25) involving the Marcum Q -function. Solid lines are exact values while crosses are the results obtained from Lemma 3 and (32). $\theta_1 = 0, \theta_2 = \infty$.

Finally, to tightly approximate the Marcum Q -function at the tails, which are the range of interest in, e.g., error probability analysis, one can use the approximation schemes of [29], [30].

III. APPLICATIONS IN PA SYSTEMS

In Section II, we showed how the proposed approximation scheme enables us to derive closed-form expressions for a broad range of integrals, as required in various expectation-based calculations, e.g., [7], [16]–[18], [29], [34], [62]. On the other hand, the Marcum Q -function may also appear in optimization problems, e.g., [19, eq. (8)], [20, eq. (9)], [21, eq. (10)], [22, eq. (10)], [23, eq. (15)], [24, eq. (22)]. For this reason, in this section, we provide an example of using our proposed semi-linear approximation in an optimization problem for the PA systems.

A. Problem Formulation

Vehicle communication is one of the most important use cases in 5G. Here, the main focus is to provide efficient and reliable connections to cars and public transports, e.g., busses and trains. CSIT plays an important role in achieving these goals, since the data transmission efficiency can be improved by updating the transmission parameters relative to the instantaneous channel state. However, the typical CSIT acquisition systems, which are mostly designed for (semi)static channels, may not work well for high-speed vehicles. This is because, depending on the vehicle speed, the position of the antennas may change quickly and the channel information becomes inaccurate. To overcome this issue, [40]–[45] propose the PA setup as shown in Fig. 4. With a PA setup, which is of interest in Vehicle-to-everything (V2X) communications [40] as well as integrated access and backhauling [63], two antennas are deployed on the top of the vehicle. The first antenna, the PA, estimates the channel and sends feedback

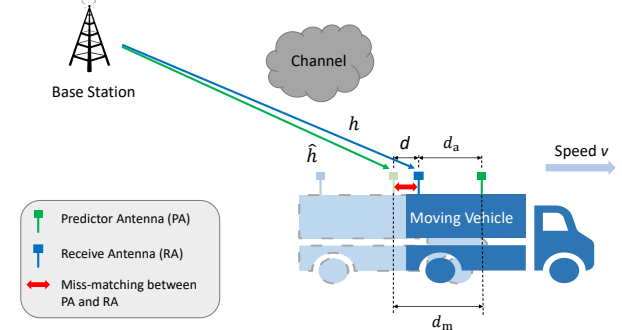


Fig. 4. A PA system with the mismatch problem. Here, \hat{h} is the channel between the BS and the PA while h refers to the BS-RA link. The vehicle is moving with speed v and the antenna separation is d_a . The red arrow indicates the spatial mismatch, i.e., when the RA does not reach at the same point as the PA when sending pilots. Also, d_m is the moving distance of the vehicle which is affected by the processing delay δ of the BS.

to the BS at time t . Then, the BS uses the CSIT provided by the PA to communicate with a second antenna, which we refer to as RA, at time $t + \delta$, where δ is the processing time at the BS. In this way, the BS can use the CSIT acquired from the PA and perform various CSIT-based transmission schemes, e.g., [40], [45].

We assume that the vehicle moves through a stationary electromagnetic standing wave pattern ². Thus, if the RA reaches exactly the same position as the position of the PA when sending the pilots, it will experience the same channel and the CSIT will be perfect. However, if the RA does not reach the same spatial point as the PA, due to, e.g., the BS processing delay is not equal to the time that we need until the RA reaches the same point as the PA, the RA may receive the data in a place different from the one in which the PA was sending the pilots. Such spatial mismatch may lead to CSIT inaccuracy, which will affect the system performance considerably. Thus, we need adaptive schemes to compensate for it.

Considering downlink transmission in the BS-RA link, the received signal is given by

$$Y = \sqrt{P}hX + Z. \quad (35)$$

Here, P represents the transmit power, X is the input message with unit variance, and h is the fading coefficient between the BS and the RA. Also, $Z \sim \mathcal{CN}(0, 1)$ denotes the independent and identically distributed (IID) complex Gaussian noise added at the receiver.

We denote the channel coefficient of the PA-BS uplink as \hat{h} . Also, we define d as the effective distance between the place where the PA estimates the channel at time t , and the place where the RA reaches at time $t + \delta$. As can be seen in Fig. 4, d can be calculated as

$$d = |d_a - d_m| = |d_a - v\delta|, \quad (36)$$

where d_m is the moving distance of the vehicle during time interval δ , and v is the velocity of the vehicle. Also, d_a is the

²This has been experimentally verified in, e.g., [64]

antenna separation between the PA and the RA. In conjunction to (36), here, we assume d can be calculated by the BS.

Using the classical Jake's correlation model [65, p. 2642] and assuming a semi-static propagation environment, i.e., assuming that the coherence time of the propagation environment is larger than δ , the channel coefficient of the BS-RA downlink can be modeled as

$$h = \sqrt{1 - \sigma^2} \hat{h} + \sigma q. \quad (37)$$

Here, $q \sim \mathcal{CN}(0, 1)$ which is independent of the known channel value $\hat{h} \sim \mathcal{CN}(0, 1)$, and σ is a function of the effective distance d as

$$\sigma = \frac{\frac{\phi_2^2 - \phi_1^2}{\phi_1}}{\sqrt{\left(\frac{\phi_2}{\phi_1}\right)^2 + \left(\frac{\phi_2^2 - \phi_1^2}{\phi_1}\right)^2}} = \frac{\phi_2^2 - \phi_1^2}{\sqrt{(\phi_2)^2 + (\phi_2^2 - \phi_1^2)^2}}. \quad (38)$$

Here, $\phi_1 = \Phi_{1,1}^{1/2}$ and $\phi_2 = \Phi_{1,2}^{1/2}$, where Φ is from Jake's model [65, p. 2642]

$$[\hat{h}] = \Phi^{1/2} \mathbf{H}_\varepsilon. \quad (39)$$

Note that, the channel model (37) has been experimentally verified in, e.g., [64] for PA setups. Also, one can follow the same method as in [48] to extend the model to the cases with temporally-correlated channels. Moreover, in (39), \mathbf{H}_ε has independent circularly-symmetric zero-mean complex Gaussian entries with unit variance, and Φ is the channel correlation matrix with the (i, j) -th entry given by

$$\Phi_{i,j} = J_0((i-j) \cdot 2\pi d/\lambda) \forall i, j. \quad (40)$$

Here, $J_n(x) = (\frac{x}{2})^n \sum_{i=0}^{\infty} \frac{(\frac{x}{2})^{2i} (-1)^i}{i! \Gamma(n+i+1)}$ represents the n -th order Bessel function of the first kind. Moreover, λ denotes the carrier wavelength, i.e., $\lambda = c/f_c$ where c is the speed of light and f_c is the carrier frequency.

From (37), for a given \hat{h} and $\sigma \neq 0$, $|h|$ follows a Rician distribution, i.e., the probability density function (PDF) of $|h|$ is given by

$$f_{|h| \mid \hat{h}}(x) = \frac{2x}{\sigma^2} e^{-\frac{x^2 + \hat{g}}{\sigma^2}} I_0\left(\frac{2x\sqrt{\hat{g}}}{\sigma^2}\right), \quad (41)$$

where $\hat{g} = (1 - \sigma^2)|\hat{h}|^2$. Let us define the channel gain between BS-RA as $g = |h|^2$. Then, the PDF of $f_{g \mid \hat{h}}$ is given by

$$f_{g \mid \hat{h}}(x) = \frac{1}{\sigma^2} e^{-\frac{x + \hat{g}}{\sigma^2}} I_0\left(\frac{2\sqrt{x\hat{g}}}{\sigma^2}\right), \quad (42)$$

which is non-central Chi-squared distributed with the CDF containing the first-order Marcum Q -function as

$$F_{g \mid \hat{h}}(x) = 1 - Q_1\left(\sqrt{\frac{2\hat{g}}{\sigma^2}}, \sqrt{\frac{2x}{\sigma^2}}\right). \quad (43)$$

B. Analytical Results on Rate Adaptation Using the Semi-Linear Approximation of the First-order Marcum Q -Function

We assume that d_a , δ and \hat{g} are known by the BS. It can be seen from (42) that $f_{g \mid \hat{h}}(x)$ is a function of v . For a given v , the distribution of g is known by the BS, and a rate adaption scheme can be performed to improve the system performance.

For a given instantaneous value of \hat{g} , the data is transmitted with instantaneous rate $R_{\mid \hat{g}}$ nats-per-channel-use (npcu). If the instantaneous channel gain realization supports the transmitted data rate $R_{\mid \hat{g}}$, i.e., $\log(1 + gP) \geq R_{\mid \hat{g}}$, the data can be successfully decoded. Otherwise, outage occurs. Hence, the outage probability in each time slot is

$$\Pr(\text{outage} \mid \hat{g}) = F_{g \mid \hat{g}}\left(\frac{e^{R_{\mid \hat{g}}} - 1}{P}\right). \quad (44)$$

Also, the instantaneous throughput for a given \hat{g} is

$$\eta_{\mid \hat{g}}(R_{\mid \hat{g}}) = R_{\mid \hat{g}} (1 - \Pr(\log(1 + gP) < R_{\mid \hat{g}})), \quad (45)$$

and the optimal rate adaptation maximizing the instantaneous throughput is obtained by

$$\begin{aligned} R_{\mid \hat{g}}^{\text{opt}} &= \underset{R_{\mid \hat{g}} \geq 0}{\text{argmax}} \{ (1 - \Pr(\log(1 + gP) < R_{\mid \hat{g}})) R_{\mid \hat{g}} \} \\ &= \underset{R_{\mid \hat{g}} \geq 0}{\text{argmax}} \left\{ \left(1 - F_{g \mid \hat{g}}\left(\frac{e^{R_{\mid \hat{g}}} - 1}{P}\right) \right) R_{\mid \hat{g}} \right\} \\ &= \underset{R_{\mid \hat{g}} \geq 0}{\text{argmax}} \left\{ Q_1\left(\sqrt{\frac{2\hat{g}}{\sigma^2}}, \sqrt{\frac{2(e^{R_{\mid \hat{g}}} - 1)}{P\sigma^2}}\right) R_{\mid \hat{g}} \right\}, \end{aligned} \quad (46)$$

where the last equality comes from (43).

Using the derivatives of the Marcum Q -function, (46) does not have a closed-form solution³. For this reason, Lemma 4 uses the semi-linear approximation scheme of Lemma 1 and Corollaries 1-2 to find the optimal data rate maximizing the instantaneous throughput.

Lemma 4. *For a given channel realization \hat{g} , the throughput-optimized rate allocation is approximately given by (49) where $\mathcal{W}(\cdot)$ denotes the Lambert \mathcal{W} -function.*

Proof. The approximation results of Lemma 1 and Corollaries 1-2 can be generalized by $y(\alpha, \beta) \simeq \tilde{\mathcal{Z}}_{\text{general}}(\alpha, \beta)$ where

$$\tilde{\mathcal{Z}}_{\text{general}}(\alpha, \beta) \simeq \begin{cases} 0, & \text{if } \beta < c_1(\alpha) \\ o_1(\alpha)(\beta - o_2(\alpha)) + o_3, & \text{if } c_1(\alpha) \leq \beta \leq c_2(\alpha) \\ 1, & \text{if } \beta > c_2(\alpha). \end{cases} \quad (47)$$

o_i , $i = 1, 2, 3$, are given by (2), (13), or (20) depending on if we use Lemma 1 or Corollaries 1-2. In this way, (45) is approximated as

$$\eta_{\mid \hat{g}} \simeq R_{\mid \hat{g}} (1 - o_1(\alpha)\beta + o_1(\alpha)o_2(\alpha) - o_3(\alpha)), \quad (48)$$

³To solve (46), one can use different approximation methods of the Marcum Q -function, e.g., [48]. Here, we use Lemma 1/Corollaries 1-2 to solve (46) to show the usefulness of the semi-linear approximation method. As shown, in Figs. 5 and 6, the semi-linear approximation is tight for a broad range of parameter settings while it simplifies the optimization problem considerably.

where $\alpha = \sqrt{\frac{2\hat{g}}{\sigma^2}}$. To simplify the equation, we omit α in the following since it is a constant for given \hat{g} , σ . Then, setting the derivative of (48) equal to zero, we obtain

$$\begin{aligned} R_{|\hat{g}}^{\text{opt}} &= \arg \underset{R_{|\hat{g}} \geq 0}{\left\{ 1 + o_1 o_2 - o_3 - o_1 \left(\frac{(R_{|\hat{g}} + 2)e^{R_{|\hat{g}}} - 2}{\sqrt{2P\sigma^2 (e^{R_{|\hat{g}}} - 1)}} \right) = 0 \right\}} \\ &\stackrel{(b)}{\approx} \arg \underset{R_{|\hat{g}} \geq 0}{\left\{ \left(\frac{R_{|\hat{g}} + 1}{2} \right) e^{\frac{R_{|\hat{g}}}{2} + 1} = \frac{(1 + o_1 o_2 - o_3)e\sqrt{2P\sigma^2}}{2o_1} \right\}} \\ &\stackrel{(c)}{=} 2\mathcal{W} \left(\frac{(1 + o_1 o_2 - o_3)e\sqrt{2P\sigma^2}}{2o_1} - 1 \right). \end{aligned} \quad (49)$$

Here, (b) comes from $e^{R_{|\hat{g}}} - 1 \simeq e^{R_{|\hat{g}}}$ and $(R_{|\hat{g}} + 2)e^{R_{|\hat{g}}} - 2 \simeq (R_{|\hat{g}} + 2)e^{R_{|\hat{g}}}$ which are appropriate at moderate/high values of $R_{|\hat{g}}$. Also, (c) is obtained by the definition of the Lambert \mathcal{W} -function $xe^x = y \Leftrightarrow x = \mathcal{W}(y)$ [66]. \blacksquare

Finally, the expected throughput, averaged over multiple time slots, is obtained by $\eta = \mathbb{E} \left\{ \eta |\hat{g}(R_{|\hat{g}}^{\text{opt}}) \right\}$ with expectation over \hat{g} .

Using (49) and the approximation [67, Them. 2.1]

$$\mathcal{W}(x) \simeq \log(x) - \log \log(x), x \geq 0, \quad (50)$$

we obtain

$$\begin{aligned} R_{|\hat{g}}^{\text{opt}} &\simeq 2 \log \left(\frac{(1 + o_1 o_2 - o_3)e\sqrt{2P\sigma^2}}{2o_1} - 1 \right) - \\ &\quad 2 \log \log \left(\frac{(1 + o_1 o_2 - o_3)e\sqrt{2P\sigma^2}}{2o_1} - 1 \right) \end{aligned} \quad (51)$$

which implies as the transmit power increases, the optimal instantaneous rate increases with the square root of the transmit power (approximately) logarithmically.

C. On the Effect of Imperfect Channel Estimation

In Section III-B, we assumed perfect channel estimation at the BS. The deviations of channel estimation, due to, e.g., radio-frequency mismatch, could invalidate the assumption of perfect channel estimation, and should be considered in the system design. Here, we follow the similar approach as in, e.g., [68], to add the effect of estimation error of \hat{h} as an independent additive Gaussian variable whose variance is given by the accuracy of channel estimation.

Let us define \tilde{h} as the estimate of \hat{h} at the BS. Then, we further develop our channel model (37) as

$$\tilde{h} = \kappa \hat{h} + \sqrt{1 - \kappa^2} z, \quad (52)$$

for each time slot, where $z \sim \mathcal{CN}(0, 1)$ is a Gaussian noise which is uncorrelated with H_k . Also, κ is a known correlation factor which represents the estimation error of \hat{h} by $\kappa = \frac{\mathbb{E}\{\tilde{h}\hat{h}^*\}}{\mathbb{E}\{\|\hat{h}\|^2\}}$. Substituting (52) into (37), we have

$$h = \kappa \sqrt{1 - \sigma^2} \hat{h} + \kappa \sigma q + \sqrt{1 - \kappa^2} z. \quad (53)$$

Then, because $\kappa \sigma q + \sqrt{1 - \kappa^2} z$ is equivalent to a new Gaussian variable $w \sim \mathcal{CN}(0, (\kappa \sigma)^2 + 1 - \kappa^2)$, we can follow the same procedure as in (46)-(49) to analyze the system performance with imperfect channel estimation of the PA (see Figs. 5-6 for more discussions).

D. Simulation Results

In this part, we study the performance of the PA system and verify the tightness of the approximation scheme of Lemma 4. Particularly, we present the average throughput and the outage probability of the PA setup for different vehicle speeds/channel estimation errors. As an ultimate upper bound for the proposed rate adaptation scheme, we consider a genie-aided setup where we assume that the BS has perfect CSIT of the BS-RA link without uncertainty/outage probability. Then, as a lower-bound of the system performance, we consider the cases with no CSIT/rate adaptation as shown in Fig. 5. Here, the simulation results for the cases of no adaptation are obtained with only one antenna and no CSIT. In this case, the data is sent with a fixed rate R and it is decoded if $R < \log(1 + gP)$, i.e., $g > \frac{e^R - 1}{P}$. In this way, assuming Rayleigh fading, the average rate is given by

$$R^{\text{No-adaptation}} = \int_{\frac{e^R - 1}{P}}^{\infty} Re^{-x} dx = Re^{-\frac{e^R - 1}{P}}, \quad (54)$$

and the optimal rate allocation is found by setting the derivative of (54) with respect to R equal to zero leading to $\hat{R} = \mathcal{W}(P)$, and the throughput is calculated as

$$\eta^{\text{No-adaptation}} = \mathcal{W}(P) e^{-\frac{e^{\mathcal{W}(P)} - 1}{P}}. \quad (55)$$

Also, in the simulations, we set $f_c = 2.68$ GHz and $d_a = 1.5\lambda$. Finally, each point in the figures is obtained by averaging the system performance over 1×10^5 channel realizations.

In Fig. 5, we show the expected throughput η in different cases for a broad range of signal-to-noise ratios (SNRs). Here, because the noise has unit variance, we define the SNR as $10 \log_{10} P$. Also, we set $v = 114$ km/h in Fig. 5 as defined in (36), and $\kappa = 1$ as discussed in (53). The analytical results obtained by Lemma 4 and Corollary 2, i.e., the approximation of (46), are also presented. We have also checked the approximation result of Lemma 4 while using Lemma 1/Corollary 1. Then, because the results are similar as those presented in Fig. 5, they are not included in the figure. Moreover, the figure shows the results of (55) with no CSIT/rate adaptation as a benchmark. Finally, Fig. 6 studies the expected throughput η for different values of estimation error variance κ with SNR = 10, 19, 25 dB, in the case of partial CSIT. Also, the figure evaluates the tightness of the approximation results obtained by Lemma 4. Here, we set $v = 114.5$ km/h and $\delta = 5$ ms.

Setting SNR = 23 dB and $v = 120, 150$ km/h in Fig. 7, we study the effect of the processing delay δ on the throughput. Finally, the outage probability is evaluated in Fig. 8, where the results are presented for different speeds with SNR = 10 dB, in the case of partial CSIT. Also, we present the outage probability for $\delta = 5.35$ ms and $\delta = 4.68$ ms in Fig. 8.

From the figures, we can conclude the following points:

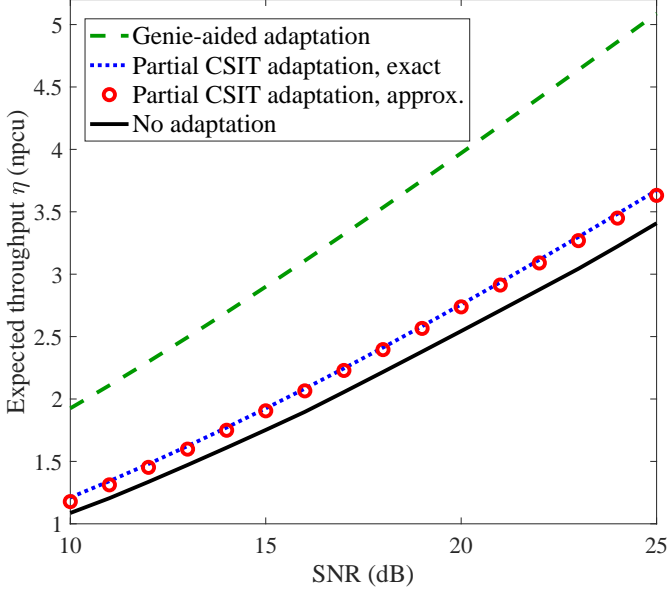


Fig. 5. Expected throughput η in different cases, $v = 114$ km/h, $\kappa = 1$, and $\delta = 5$ ms. Both the exact values estimated from simulations as well as the analytical approximations from Lemma 4 are presented.

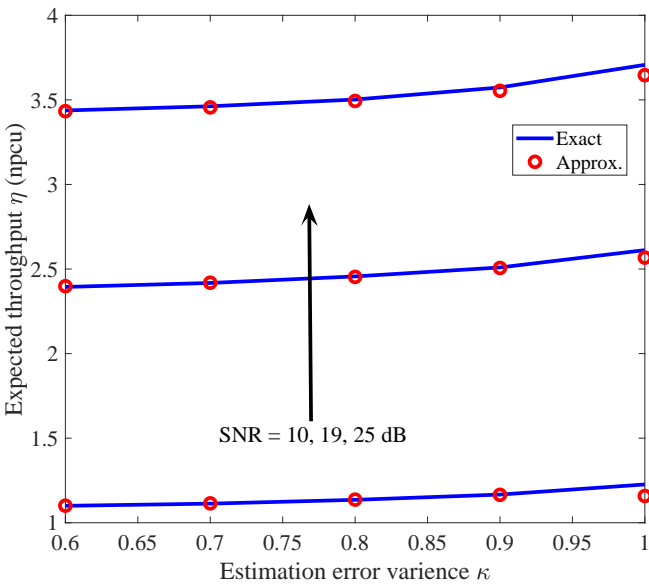


Fig. 6. Expected throughput η for different estimation errors κ with SNR = 10, 19, 25 dB, in the case of partial CSIT, exact and approximation, $v = 114.5$ km/h, and $\delta = 5$ ms. Both the exact values estimated from simulations as well as the analytical approximations from Lemma 4 are presented.

- The approximation scheme of Lemma 4 is tight for a broad range of parameter settings (Figs. 5, 6). Thus, the throughput-optimized rate allocation can be well approximated by (49), and the semi-linear approximation of Lemma 1/Corollaries 1-2 is a good approach to study the considered optimization problem.
- With deployment of the PA, remarkable throughput gain is achieved especially in moderate/high SNRs (Fig. 5). Also, the throughput decreases when the estimation error is considered, i.e., κ decreases. Finally, as can be seen in Figs. 5, 6, with rate adaptation, and without optimizing

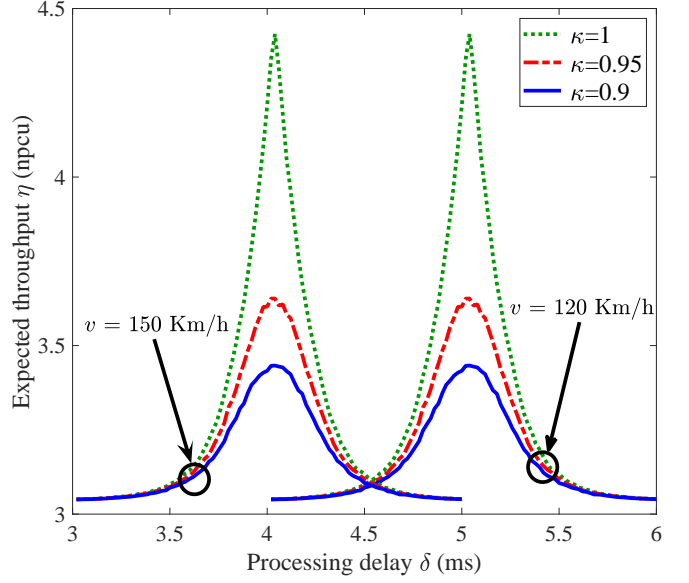


Fig. 7. Expected throughput η for different processing delays with SNR = 23 dB and $v = 120, 150$ km/h in the case of partial adaptation.

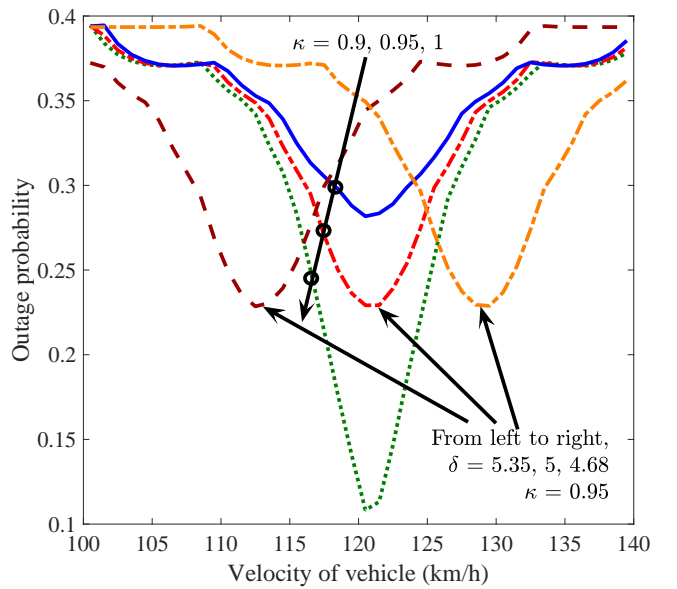


Fig. 8. Outage probability for different velocities with SNR = 10 dB, in the case of partial CSIT.

the processing delay/vehicle speed, the effect of estimation error on expected throughput is small unless for large values of κ .

- As it can be seen in Figs. 7 and 8, for different channel estimation errors, there are optimal values for the vehicle speed and the BS processing delay optimizing the system throughput and outage probability. Note that the presence of the optimal speed/processing delay can be proved via (36) as well. Finally, the optimal value of the vehicle speed, in terms of throughput/outage probability, decreases with the processing delay. However, the optimal vehicle speed/processing delay, in terms of throughput/outage probability, is almost insensitive to the

channel estimation error.

- With perfect channel estimation, the throughput/outage probability is sensitive to the speed variation, if we move away from the optimal speed (Figs. 7 and 8). However, the sensitivity to the speed/processing delay variation decreases as the channel estimation error increases, i.e., κ decreases (Figs. 7 and 8). Finally, considering Figs. 7 and 8, it is expected that adapting the processing delay, as a function of the vehicle speed, and implementing hybrid automatic repeat request protocols can improve the performance of the PA system. These points will be studied in our future works.

IV. CONCLUSION

We derived a simple semi-linear approximation method for the first-order Marcum Q -function, as one of the functions of interest in different problem formulations of wireless networks. As we showed through various analysis, while the proposed approximation is not tight at the tails of the function, it is useful in different optimization- and expectation-based problem formulations. Particularly, as an application of interest, we used the proposed approximation to analyze the performance of PA setups using rate adaptation. As we showed, with different levels of channel estimation error/processing delay, adaptive rate allocation can effectively compensate for the spatial mismatch problem, and improve the throughput/outage probability of PA networks. It is expected that increasing the number of RA antennas will improve the performance of the PA system considerably.

APPENDIX A PROOF OF LEMMA 2

Using Corollary 1, we have

$$G(\alpha, \rho) \simeq \begin{cases} \int_{\rho}^{\check{c}_1} 0dx + \int_{\check{c}_1}^{\check{c}_2} e^{-nx} x^m \times \\ \left(\frac{1}{\sqrt{2\pi}}(x - \alpha) + \frac{1}{2} \left(1 - \frac{1}{\sqrt{2\pi\alpha^2}} \right) \right) dx + \\ \int_{\check{c}_2}^{\infty} e^{-nx} x^m dx, & \text{if } \rho < \check{c}_1 \\ \int_{\rho}^{\check{c}_2} e^{-nx} x^m \times \\ \left(\frac{1}{\sqrt{2\pi}}(x - \alpha) + \frac{1}{2} \left(1 - \frac{1}{\sqrt{2\pi\alpha^2}} \right) \right) dx + \\ \int_{\check{c}_2}^{\infty} e^{-nx} x^m dx, & \text{if } \check{c}_1 \leq \rho < \check{c}_2, \\ \int_{\rho}^{\infty} e^{-nx} x^m dx, & \text{if } \rho \geq \check{c}_2. \end{cases}$$

Then, for $\rho \geq \check{c}_2$, we obtain

$$\begin{aligned} & \int_{\rho}^{\infty} e^{-nx} \times x^m (1 - Q_1(\alpha, x)) dx \\ & \stackrel{(d)}{\simeq} \int_{\rho}^{\infty} e^{-nx} \times x^m dx \stackrel{(e)}{=} \Gamma(m+1, n\rho) n^{-m-1}, \end{aligned} \quad (56)$$

while for $\rho < \check{c}_2$, we have

$$\begin{aligned} & \int_{\rho}^{\infty} e^{-nx} \times x^m (1 - Q_1(\alpha, x)) dx \\ & \stackrel{(f)}{\simeq} \int_{\max(\check{c}_1, \rho)}^{\check{c}_2} \left(\frac{1}{\sqrt{2\pi}}(x - \alpha) + \frac{1}{2} \left(1 - \frac{1}{\sqrt{2\pi\alpha^2}} \right) \right) \times \\ & \quad e^{-nx} x^m dx + \int_{\check{c}_2}^{\infty} e^{-nx} x^m dx \\ & \stackrel{(g)}{=} \Gamma(m+1, n\check{c}_2) n^{-m-1} + \\ & \quad \left(-\frac{\alpha}{\sqrt{2\pi}} + 0.5 * \left(1 - \frac{1}{\sqrt{2\pi\alpha^2}} \right) \right) \times n^{-m-1} \times \\ & \quad (\Gamma(m+1, n\max(\check{c}_1, \rho)) - \Gamma(m+1, n\check{c}_2)) + \\ & \quad (\Gamma(m+2, n\max(\check{c}_1, \rho)) - \Gamma(m+2, n\check{c}_2)) \frac{n^{-m-2}}{\sqrt{2\pi}}. \end{aligned} \quad (57)$$

Note that (d) and (f) come from Corollary 1 while (e) and (g) use the fact that $\Gamma(s, x) \rightarrow 0$ as $x \rightarrow \infty$.

APPENDIX B PROOF OF LEMMA 3

Using Lemma 1, the integral (25) can be approximated as

- for $\theta_2 > \theta_1 > c_2$, $T(\alpha, m, a, \theta_1, \theta_2) \simeq 0$,

2) for $c_1 < \theta_1 \leq c_2, \theta_2 > \theta_1$,

$$T(\alpha, m, a, \theta_1, \theta_2) = \int_{\theta_1}^{\min(c_2, \theta_2)} (n_2 x + n_1) e^{-mx} \log(1 + ax) dx, \quad (58)$$

3) for $\theta_1 < c_1, \theta_2 > c_1$,

$$\begin{aligned} T(\alpha, m, a, \theta_1, \theta_2) & \simeq \int_{\theta_1}^{c_1} e^{-mx} \log(1 + ax) dx + \\ & \int_{c_1}^{\min(c_2, \theta_2)} (n_2 x + n_1) e^{-mx} \log(1 + ax) dx, \end{aligned} \quad (59)$$

4) for $\theta_1 < \theta_2 < c_1$,

$$T(\alpha, m, a, \theta_1, \theta_2) \simeq \int_{\theta_1}^{\theta_2} e^{-mx} \log(1 + ax) dx. \quad (60)$$

Then, consider case 3 where

$$\begin{aligned} T(\alpha, m, a, \theta_1, \theta_2) & = \int_{\theta_1}^{\theta_2} e^{-mx} \log(1 + ax) Q_1(\alpha, x) dx \\ & \simeq \int_{\theta_1}^{c_1} e^{-mx} \log(1 + ax) dx + \\ & \quad \int_{c_1}^{\theta_2} (n_2 x + n_1) e^{-mx} \log(1 + ax) dx \\ & = \mathcal{F}_1(c_1) - \mathcal{F}_1(\theta_1) + \mathcal{F}_2(\theta_2) - \mathcal{F}_2(c_1), \end{aligned} \quad (61)$$

with n_1 and n_2 being functions of the constant α and given by (29) and (30), respectively. Here, we assume $\theta_1 < c_1$ and $c_2 > \theta_2 > c_1$ for simplicity. The other cases can be proved

with the same procedure. Moreover, the functions $\mathcal{F}_1(x)$ and $\mathcal{F}_2(x)$ are obtained by

$$\begin{aligned}\mathcal{F}_1(x) &= \int e^{-mx} \log(1+ax) dx \\ &\stackrel{(h)}{=} -\frac{e^{-mx} \log(ax+1)}{m} - \int -\frac{ae^{-mx}}{m(ax+1)} dx \\ &\stackrel{(i)}{=} \frac{1}{m} \left(-e^{\frac{m}{a}} \text{E}_1 \left(mx + \frac{m}{a} \right) - e^{-mx} \log(ax+1) \right) + C,\end{aligned}\quad (62)$$

and

$$\begin{aligned}\mathcal{F}_2(x) &= \int (n_2 x + n_1) e^{-mx} \log(1+ax) dx \\ &\stackrel{(j)}{=} -\frac{(mn_2 x + n_2 + mn_1) e^{-mx} \log(1+ax)}{m^2} - \\ &\quad \int \frac{a(-mn_2 x - n_2 - mn_1) e^{-mx}}{m^2(ax+1)} dx \\ &\stackrel{(k)}{=} -\frac{(mn_2 x + n_2 + mn_1) e^{-mx} \log(1+ax)}{m^2} - \\ &\quad - \frac{1}{a} \left(e^{\frac{m}{a}} (mn_2 x + n_2 + mn_1) \right. \\ &\quad \left. \text{E}_1 \left(mx + \frac{m}{a} \right) \right) + \int -\frac{m e^{\frac{m}{a}} n_2}{\text{E}_1 \left(mx + \frac{m}{a} \right)} dx \\ &\stackrel{(l)}{=} -\frac{(mn_2 x + n_2 + mn_1) e^{-mx} \log(1+ax)}{m^2} - \\ &\quad - \frac{1}{a} \left(e^{\frac{m}{a}} (mn_2 x + n_2 + mn_1) \text{E}_1 \left(mx + \frac{m}{a} \right) \right) + \\ &\quad \frac{n_2 e^{-mx}}{a} - \frac{e^{\frac{m}{a}} n_2 (mx + \frac{m}{a}) \text{E}_1 \left(mx + \frac{m}{a} \right)}{a} + C,\end{aligned}\quad (63)$$

where (h), (j) and (k) come from partial integration and some manipulations. Also, (i) and (l) use [69, p. 195]

$$\int \text{E}_1(u) du = u \text{E}_1(u) - e^{-u}. \quad (64)$$

REFERENCES

- [1] M. Z. Bocus, C. P. Dettmann, and J. P. Coon, "An approximation of the first order Marcum Q -function with application to network connectivity analysis," *IEEE Commun. Lett.*, vol. 17, no. 3, pp. 499–502, Mar. 2013.
- [2] C. W. Helstrom, *Elements of Signal Detection and Estimation*. Prentice-Hall, Inc., 1994.
- [3] B. Makki and T. Eriksson, "Feedback subsampling in temporally-correlated slowly-fading channels using quantized CSI," *IEEE Trans. Commun.*, vol. 61, no. 6, pp. 2282–2294, Jun. 2013.
- [4] ———, "On the capacity of Rayleigh-fading correlated spectrum sharing networks," *Eurasip J. Wireless Commun. Netw.*, vol. 2011, no. 1, p. 83, Aug. 2011.
- [5] B. Makki, T. Svensson, K. Buisman, J. Perez, and M.-S. Alouini, "Wireless energy and information transmission in FSO and RF-FSO links," *IEEE Wireless Commun. Lett.*, vol. 7, no. 1, pp. 90–93, Feb. 2018.
- [6] B. Makki, T. Eriksson, and T. Svensson, "On the performance of the relay ARQ networks," *IEEE Trans. Veh. Technol.*, vol. 65, no. 4, pp. 2078–2096, Apr. 2016.
- [7] M. K. Simon and M.-S. Alouini, "Some new results for integrals involving the generalized Marcum Q function and their application to performance evaluation over fading channels," *IEEE Trans. Wireless Commun.*, vol. 2, no. 4, pp. 611–615, Jul. 2003.
- [8] H. A. Suraweera, P. J. Smith, and M. Shafi, "Capacity limits and performance analysis of cognitive radio with imperfect channel knowledge," *IEEE Trans. Veh. Technol.*, vol. 59, no. 4, pp. 1811–1822, May 2010.
- [9] M. Kang and M.-S. Alouini, "Largest eigenvalue of complex Wishart matrices and performance analysis of MIMO MRC systems," *IEEE J. Sel. Areas Commun.*, vol. 21, no. 3, pp. 418–426, Apr. 2003.
- [10] Y. Chen and C. Tellambura, "Distribution functions of selection combiner output in equally correlated Rayleigh, Rician, and Nakagami- m fading channels," *IEEE Trans. Commun.*, vol. 52, no. 11, pp. 1948–1956, Nov. 2004.
- [11] Y. Ma and C. Choy Chai, "Unified error probability analysis for generalized selection combining in Nakagami fading channels," *IEEE J. Sel. Areas Commun.*, vol. 18, no. 11, pp. 2198–2210, Nov. 2000.
- [12] Q. T. Zhang and H. G. Lu, "A general analytical approach to multi-branch selection combining over various spatially correlated fading channels," *IEEE Trans. Commun.*, vol. 50, no. 7, pp. 1066–1073, Jul. 2002.
- [13] A. Ghasemi and E. S. Sousa, "Spectrum sensing in cognitive radio networks: requirements, challenges and design trade-offs," *IEEE Commun. Mag.*, vol. 46, no. 4, pp. 32–39, Apr. 2008.
- [14] F. F. Digham, M.-S. Alouini, and M. K. Simon, "On the energy detection of unknown signals over fading channels," *IEEE Trans. Commun.*, vol. 55, no. 1, pp. 21–24, Jan. 2007.
- [15] M. K. Simon and M.-S. Alouini, "Digital communication over generalized fading channels: a unified approach to performance analysis," *Wiley, New York*, 2005.
- [16] K. Cao and X. Gao, "Solutions to generalized integrals involving the generalized Marcum Q -function with application to energy detection," *IEEE Commun. Lett.*, vol. 20, no. 9, pp. 1780–1783, Sep. 2016.
- [17] P. C. Sofotasios, S. Muhaidat, G. K. Karagiannidis, and B. S. Sharif, "Solutions to integrals involving the Marcum Q -function and applications," *IEEE Signal Process. Lett.*, vol. 22, no. 10, pp. 1752–1756, Oct. 2015.
- [18] G. Cui, L. Kong, X. Yang, and D. Ran, "Two useful integrals involving generalised Marcum Q -function," *Electron. Lett.*, vol. 48, no. 16, pp. 1017–1018, Aug. 2012.
- [19] M. M. Azari, F. Rosas, K. Chen, and S. Pollin, "Ultra reliable UAV communication using altitude and cooperation diversity," *IEEE Trans. Commun.*, vol. 66, no. 1, pp. 330–344, Jan. 2018.
- [20] M. M. Alam, S. Bhattacharai, L. Hong, and S. Shetty, "Robust transmit beamforming against steering vector uncertainty in cognitive radio networks," in *Proc. IEEE INFOCOMW*, Apr. 2014, pp. 700–705.
- [21] B. Gao, M. Lin, K. An, G. Zheng, L. Zhao, and X. Liu, "ADMM-based optimal power control for cognitive satellite terrestrial uplink networks," *IEEE Access*, vol. 6, pp. 64 757–64 765, Oct. 2018.
- [22] H. Shen, W. Xu, and C. Zhao, "Outage minimized full-duplex multi-antenna DF relaying with CSI uncertainty," *IEEE Trans. Veh. Technol.*, vol. 67, no. 9, pp. 9000–9005, Sep. 2018.
- [23] T. Song, Q. Wang, M. Wu, T. Ohtsuki, M. Gurusamy, and P. Kam, "Impact of pointing errors on the error performance of intersatellite laser communications," *J. Lightw. Technol.*, vol. 35, no. 14, pp. 3082–3091, Jul. 2017.
- [24] H. Tang, L. Chai, and X. Wan, "An augmented generalized likelihood ratio test detector for signal detection in clutter and noise," *IEEE Access*, vol. 7, pp. 163 478–163 486, Nov. 2019.
- [25] N. Y. Ermolova and O. Tirkkonen, "Laplace transform of product of generalized Marcum Q , Bessel I, and power functions with applications," *IEEE Trans. Signal Process.*, vol. 62, no. Nov., pp. 2938–2944, 4 2014.
- [26] K. P. Peppas, G. C. Alexandropoulos, and P. T. Mathiopoulos, "Performance analysis of dual-hop AF relaying systems over mixed η - μ and κ - μ fading channels," *IEEE Trans. Veh. Technol.*, vol. 62, no. 7, pp. 3149–3163, Mar. 2013.
- [27] H. Fu and P. Kam, "Exponential-type bounds on the first-order Marcum Q -function," in *Proc. IEEE GLOBECOM*, Houston, Texas, USA, Dec. 2011, pp. 1–5.
- [28] X. Zhao, D. Gong, and Y. Li, "Tight geometric bound for Marcum Q -function," *Electron. Lett.*, vol. 44, no. 5, pp. 340–341, Feb. 2008.
- [29] M. K. Simon and M.-S. Alouini, "Exponential-type bounds on the generalized Marcum Q -function with application to error probability analysis over fading channels," *IEEE Trans. Commun.*, vol. 48, no. 3, pp. 359–366, Mar. 2000.
- [30] A. Annamalai and C. Tellambura, "Cauchy–Schwarz bound on the generalized Marcum Q -function with applications," *Wireless Commun. Mob. Comput.*, vol. 1, no. 2, pp. 243–253, Apr. 2001.
- [31] P. C. Sofotasios and S. Freear, "Novel expressions for the Marcum and one dimensional Q -functions," in *Proc. IEEE ISWCS*, York, United Kingdom, Sep. 2010, pp. 736–740.
- [32] R. Li, P. Y. Kam, and H. Fu, "New representations and bounds for the generalized Marcum Q -function via a geometric approach, and an

application," *IEEE Trans. Commun.*, vol. 58, no. 1, pp. 157–169, Jan. 2010.

[33] S. András, A. Baricz, and Y. Sun, "The generalized Marcum Q-function: an orthogonal polynomial approach," *Acta Universitatis Sapientiae Mathematica*, vol. 3, no. 1, pp. 60–76, Oct. 2011.

[34] S. Gaur and A. Annamalai, "Some integrals involving the $Q_m(a\sqrt{x}, b\sqrt{x})$ with application to error probability analysis of diversity receivers," *IEEE Trans. Veh. Technol.*, vol. 52, no. 6, pp. 1568–1575, Nov. 2003.

[35] P. Y. Kam and R. Li, "Computing and bounding the first-order Marcum Q-function: a geometric approach," *IEEE Trans. Commun.*, vol. 56, no. 7, pp. 1101–1110, Jul. 2008.

[36] G. E. Corazza and G. Ferrari, "New bounds for the Marcum Q-function," *IEEE Trans. Inf. Theory*, vol. 48, no. 11, pp. 3003–3008, Nov. 2002.

[37] Á. Baricz and Y. Sun, "New bounds for the generalized Marcum Q-function," *IEEE Trans. Inf. Theory*, vol. 55, no. 7, pp. 3091–3100, Jul. 2009.

[38] M. Chiani, "Integral representation and bounds for Marcum Q-function," *Electron. Lett.*, vol. 35, no. 6, pp. 445–446, Mar. 1999.

[39] D. Morales-Jimenez, F. J. Lopez-Martinez, E. Martos-Naya, J. F. Paris, and A. Lozano, "Connections between the generalized Marcum Q-function and a class of Hypergeometric functions," *IEEE Trans. Inf. Theory*, vol. 60, no. 2, pp. 1077–1082, Nov. 2014.

[40] M. Sternad, M. Grieger, R. Apelfröjd, T. Svensson, D. Aronsson, and A. B. Martinez, "Using predictor antennas for long-range prediction of fast fading for moving relays," in *Proc. IEEE WCNCW*, Paris, France, Apr. 2012, pp. 253–257.

[41] D.-T. Phan-Huy, M. Sternad, and T. Svensson, "Making 5G adaptive antennas work for very fast moving vehicles," *IEEE Intell. Transp. Syst. Mag.*, vol. 7, no. 2, pp. 71–84, Apr. 2015.

[42] J. Björsell, M. Sternad, and M. Grieger, "Predictor antennas in action," in *Proc. IEEE PIMRC*, Montreal, Quebec, Canada, Oct. 2017, pp. 1–7.

[43] D.-T. Phan-Huy, S. Wesemann, J. Bjoersell, and M. Sternad, "Adaptive massive MIMO for fast moving connected vehicles: It will work with predictor antennas!" in *Proc. 22nd Int. ITG Workshop Smart Antennas (WSA) '2018*, Bochum, Germany, Mar. 2018, pp. 1–8.

[44] N. Jamaly, R. Apelfröjd, A. Belen Martinez, M. Grieger, T. Svensson, M. Sternad, and G. Fettweis, "Analysis and measurement of multiple antenna systems for fading channel prediction in moving relays," in *Proc. IEEE EuCAP*, The Hague, The Netherlands, Apr. 2014, pp. 2015–2019.

[45] J. Björsell, M. Sternad, and M. Grieger, "Using predictor antennas for the prediction of small-scale fading provides an order-of-magnitude improvement of prediction horizons," in *Proc. IEEE ICCW*, Paris, France, May 2017, pp. 54–60.

[46] R. Apelfröjd, J. Björsell, M. Sternad, and D. Phan-Huy, "Kalman smoothing for irregular pilot patterns; a case study for predictor antennas in TDD systems," in *Proc. IEEE PIMRC*, Bologna, Italy, Sep. 2018, pp. 1–7.

[47] N. Jamaly, T. Svensson, and A. Derneryd, "Effects of coupling and overspeeding on performance of predictor antenna systems in wireless moving relays," *IET Microw., Antennas Propag.*, vol. 13, no. 3, pp. 367–372, Feb. 2019.

[48] H. Guo, B. Makki, and T. Svensson, "Rate adaptation in predictor antenna systems," *IEEE Wireless Commun. Lett.*, vol. 9, no. 4, pp. 448–451, Apr. 2020.

[49] T. Ekman, "Predictions of mobile radio channels," Ph.D. dissertation, Uppsala University, Uppsala, Sweden, Oct. 2002.

[50] D. Aronsson, "Channel estimation and prediction for MIMO OFDM systems - Key design and Performance Aspects of Kalman-based Algorithms," Ph.D. dissertation, Uppsala University, Uppsala, Sweden, Mar. 2011.

[51] EU ARTIST4G Project, "Deliverable D3.5c-Moving relays and mobility aspects," May 2012, available at https://www.researchgate.net/publication/266141186_EU_FP7_INFOSO-ICT-247223_ARTIST4G_Project_Deliverable_D35c_Moving_Relays_and_Mobility_aspects.

[52] EU METIS Project, "Deliverable D3.3-Final performance results and consolidated view on the most promising multi-node/multi-antenna transmission technologies," Feb. 2015, available at https://metis2020.com/wp-content/uploads/deliverables/METIS_D3.3_v1.pdf.

[53] EU 5GCAR Project, "Deliverable D3.3-Final 5G V2X Radio Design," May 2019, available at https://5gcar.eu/wp-content/uploads/2019/06/5GCAR_D3.3_v1.0.pdf.

[54] H. Guo, B. Makki, M.-S. Alouini, and T. Svensson, "Power allocation in HARQ-based predictor antenna systems," Apr. 2020, available at <https://arxiv.org/abs/2004.01421>.

[55] ———, "On delay-limited average rate of HARQ-based predictor antenna systems," Apr. 2020, available at <https://arxiv.org/abs/2004.01423>.

[56] W. K. Pratt, "Partial differentials of Marcum's Q function," *Proc. IEEE*, vol. 56, no. 7, pp. 1220–1221, Jul. 1968.

[57] M. S. Abramowitz and I. Stegun, "Handbook of Mathematical Functions with Formulas, Graphs, and Mathematical Tables," New York: Dover, 1972.

[58] M. Schwartz, W. R. Bennett, and S. Stein, *Communication Systems and Techniques*. John Wiley & Sons, 1995.

[59] E. Biglieri, J. Proakis, and S. Shamai, "Fading channels: information-theoretic and communications aspects," *IEEE Trans. Inf. Theory*, vol. 44, no. 6, pp. 2619–2692, Oct. 1998.

[60] S. Verdú and Te Sun Han, "A general formula for channel capacity," *IEEE Trans. Inf. Theory*, vol. 40, no. 4, pp. 1147–1157, Jul. 1994.

[61] B. Makki and T. Eriksson, "On the performance of MIMO-ARQ systems with channel state information at the receiver," *IEEE Trans. Commun.*, vol. 62, no. 5, pp. 1588–1603, May 2014.

[62] P. C. Sofotasios, T. A. Tsiftsis, Y. A. Brychkov, S. Freear, M. Valkama, and G. K. Karagiannidis, "Analytic expressions and bounds for special functions and applications in communication theory," *IEEE Trans. Inf. Theory*, vol. 60, no. 12, pp. 7798–7823, Dec. 2014.

[63] O. Teyeb, A. Muhammad, G. Mildh, E. Dahlman, F. Barac, and B. Makki, "Integrated Access Backhauled Networks," in *Proc. IEEE VTC-Fall*, Honolulu, HI, USA, Sep. 2019, pp. 1–5.

[64] N. Jamaly, R. Apelfröjd, A. Belen Martinez, M. Grieger, T. Svensson, M. Sternad, and G. Fettweis, "Analysis and measurement of multiple antenna systems for fading channel prediction in moving relays," in *Proc. IEEE EuCAP*, Hague, Netherlands, Apr. 2014, pp. 2015–2019.

[65] H. Shin and J. H. Lee, "Capacity of multiple-antenna fading channels: spatial fading correlation, double scattering, and keyhole," *IEEE Trans. Inf. Theory*, vol. 49, no. 10, pp. 2636–2647, Oct. 2003.

[66] R. M. Corless, G. H. Gonnet, D. E. Hare, D. J. Jeffrey, and D. E. Knuth, "On the Lambert W function," *Advances in Computational Mathematics*, vol. 5, no. 1, pp. 329–359, Dec. 1996.

[67] A. Hoofar and M. Hassani, "Approximation of the Lambert \mathcal{W} -function and hyperpower function," *Research report collection*, vol. 10, no. 2, 2007.

[68] C. Wang, E. K. S. Au, R. D. Murch, W. H. Mow, R. S. Cheng, and V. Lau, "On the performance of the MIMO zero-forcing receiver in the presence of channel estimation error," *IEEE Trans. Wireless Commun.*, vol. 6, no. 3, pp. 805–810, Mar. 2007.

[69] M. Geller and E. W. Ng, "A table of integrals of the exponential integral," *Journal of Research of the National Bureau of Standards*, vol. 37B, no. 3, pp. 191–210, Mar. 1969.